Novel Ethernet Based Optical Local Area Networks for Computer Interconnection

Igor Radovanović, Wim van Etten, Robert O. Taniman, Ronny Kleinkiskamp
University of Twente
Telecommunication Engineering Group
POBOX 217, 7500AE Enschede, The Netherlands
i.radovanovic@ieee.org

Abstract

In this paper we present new optical local area networks for fiber-to-the-desk application. Presented networks are expected to bring a solution for having optical fibers all the way to computers. To bring the overall implementation costs down we have based our networks on short-wavelength optical components, multimode optical fibers, multimode polymer-based integrated-optic devices and widely used Fast Ethernet protocol. A new Physical Layer Device that can be attached to the existing network interface card has been developed and implemented such that computers can exchange data using our new networks.

1. Introduction

Advantages of having optical fiber running all the way to computers have been known for many years [1], yet most of the computers nowadays are interconnected by means of copper-based UTP cables. The reason behind this is that costs associated with implementing optical fiber network still place a strong barrier.

The need for optical computer networks first appeared in environments where interfering electromagnetic radiation strongly affects network performance resulting in long packet delay and inherently low throughput. These environments are, for example, power plants, airport buildings, military facilities etc. Optical fibers, on the other side, offer an excellent non-emissive transmission medium and at the same time are completely insensitive to incoming radiation.

Interest in having optical fiber all the way to PCs appeared also in the larger companies having huge importance of storage area networking, data back-up demands and sharing access of large databases [2]. These companies are willing to give priority to optical fibers when upgrading their networks since optical fibers offer larger headroom for future bandwidth increase. But, as long as the overall cost of the fiber networks stays high they are concentrated on the UTP medium.

In this paper we present two optical LAN architectures by means of which we try to minimize the costs associated with implementing optical fiber networks for computer interconnections. Both architectures are based on short-wavelength optical light sources, like Fabry-Perot LDs and VCSELs, multimode optical fibers, multimode polymer-based integrated-optic devices [3, 4] and widely used Fast Ethernet protocol [5]-[7]. All the computers are interconnected by means of the passive star coupler, avoiding the need for active repeater and switching hubs. For the first time we present how the passive star network can accomodate the Fast Ethernet protocol. We based our architectures on point-to-multipoint connections in contrast to all the other Fast Ethernet networks that use point-to-point connection.

The reason for using short wavelength components is that lasers and detectors working around 850 nm are much cheaper than lasers and detectors that work in 1.3 μm or 1.55μm regions. Moreover, using short-wavelength lasers and detectors offer us a possibility to integrate a Si photodiode with the receiver front-end using straightforward CMOS technology [8], something that will contribute to bring the total network implementation cost down. Further decrease in overall cost is achieved through the less downtime of the networks, low maintenance cost, extended geometrical spans and large headroom for future capacity increase. A new network interface card (NIC) that will enable computers to send data through presented networks is made my modifying the existing NIC for UTP-based 100BASE-T network to facilitate network realizations. To do so we have made changes only in the Physical Layer of the NIC keeping the Medium Access Control (MAC) Layer and the upper ones unaltered. For this purpose we have used NICs equipped with a Medium-Independent Interface (MII) connector that allows several different Physical Layer

Proceedings of the 28th Annual IEEE International Conference on Local Computer Networks (LCN'03)
0742-1303/03 $ 17.00 © 2003 IEEE

Devices (PLDs) to be connected to the same NIC, [9].

1. New optical LAN architectures

Our first proposal for the new optical LAN is the optically transparent network presented in Fig. 1.

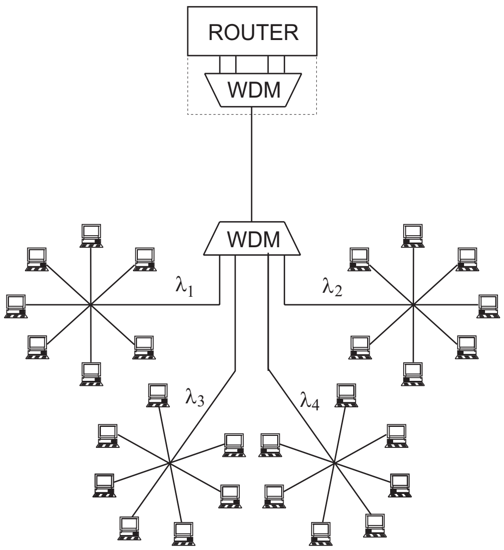

Figure 1. Optically transparent LAN for FTTD application based on multiple single-wavelength optical stars using different wavelength for each mini-star.

The segmentation of the presented network is done by means of WDM. The configuration of the network is star-shaped, segmented in mini-stars, which offers geographical advantages. Each segment of the LAN uses its own specific wavelength in the range of 790-850 nm. A common signal transfer path to the router is created by inserting a multimode coarse WDM (de)multiplexer. In this way cabling length is reduced. The stability requirements for the lasers are not so stringent since we use multimode fibers and the wavelengths are not so densely packed as in PSTN applications. The geographical spread of computers is small, so that a long common transmission line to the router is allowed. These are for example, computers of the people working on the same CAD project or application requiring exchange of large files. The electronic equipment is met only in the router, which facilitates simple maintenance. The total bandwidth is shared only among users within the same collision domain that in this architecture comprise computers in the mini-star and the router. Another advantage of this architecture is that it eanbles easy upgrade, since only the NICs at the user's site and the router has to be changed.

The disadvantages of this architecture are that NICs in computers that belong to different mini-stars require light sources emitting light at different wavelengths and the limiting span of the network since users in the mini-star and the router belong to the same collision domain, limited in length by the protocol [9, 10].

To overcome these drawbacks we have proposed another architecture that is presented in Fig. 2.

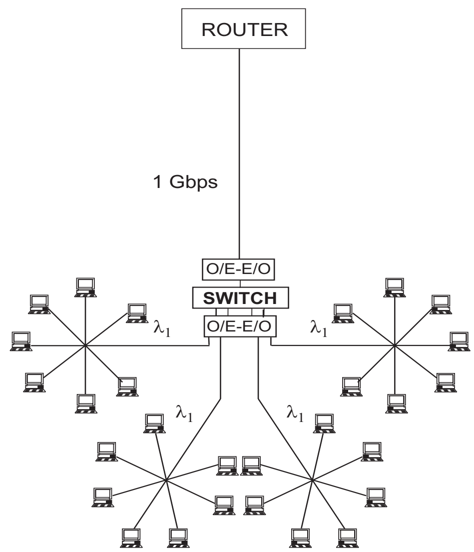

Figure 2. Optical LAN for FTTD application based on single-wavelength star using the same wavelength for each mini-star.

Here an electronic switch is introduced with a Gigabit Ethernet uplink on a single fiber pair to the router. The main advantage of this architecture is that the NICs can be identical for computers all over the LAN since all the mini-stars use the same wavelength. The network span is larger since computers in the mini-stars and the router does not belong to the same collision domain, thus the distance from computers in the mini-star to the switch can be up to 400 m. This limitation comes from the protocol itself and not from dispersion or attenuation as will be shown later in the paper.

The total bandwidth is shared only among the users within the same mini-star. The disadvantage is that electronic equipment, including power supply, must be installed outside of the router cabinet, but there is only one switch that connects all the mini-stars whereas computers are interconnected by means of the passive star coupler.

To enable the Fast Ethernet protocol to run on these networks a new NIC had to be developed. However, to

Proceedings of the 28th Annual IEEE International Conference on Local Computer Networks (LCN'03)
0742-1303/03 $ 17.00 © 2003 IEEE

facilitate network realization and decrease the overall implementation cost we have only made changes in the Physical Layer in the ISO-OSI model. MAC Layer and the upper ones remained unaltered. To achieve such implementation we have used NICs equipped with the Medium-Independent Interface (MII) connector by means of which different Physical Layer Devices (PLD) can be attached to the same NIC, [9].

A new PLD consists of the transmitter and the receiver which in turn consist of the analog and the digital circuitry. The analog circuitry has been made by using a PCB and the digital circuitry is made by using an FPGA. For designing a digital circuitry we had to take into account signals that are going from the MAC to the Physical Layer and vice versa, prescribed by the IEEE 802.3 standard [9]. Moreover in this part of the PLD transmitted data have to be processed and adapted for transmission through the fiber medium and accepted at reception from the analog part for further processing before being transfered to the MAC Layer. In the analog part of the transmitter a signal obtained from the digital part is further processed before it is used for modulation of the light source. In the receiving part conversion of optical power into an electrical signal has to be performed as well as clock and data recovery. Carrier sensing is also performed in this part, which is used for collision detection.

The main problems to be solved in designing the new PLD for presented architectures were synchronization and collision detection. These required some changes in the PLD design with respect to PLD design for the 100BASE-T networks specified in [9]. Moreover, the design of the analog and the digital part were mutually connected. For example, although the synchronization has been realized in the analog part of the PLD it affected the design of the digital part, which will be explained in Section 4.

Since both architectures are based on the passive star couplers we have a common shared medium for signal transmission inherited from the original 10BASE-T Ethernet standard in contrast to 100BASE-T Fast Ethernet where each user has a separate path to a switching hub. In the latter, synchronization is facilitated since continuous transmission between computer and a bridge or a switch can be maintained. When no packets are transmitted the IDLE signal is transmitted for synchronization. On the other side, having really a shared medium in our new architectures excludes this possibility and we had to find a solution for the synchronization of bursty traffic. The other synchronization techniques could not be used due to their long acquisition time. For example, the fastest PLL integarted circuits available on the market had acquisition time of 1 μs which is much longer that the preamble duration.

Another problem to be solved was the collision detection. In the existing 100BASE-T medium specification, collision detection has been performed in the digital part of the PLD and is based on detection of simultaneous transmission and reception of the signals. In our proposals we could use a similar approach but the problem is that the received data cannot be recovered at the beginning of the packet without being synchronized and that would have caused a large delay in the collision detection process decreasing the network throughput.

Collision detection has been solved by using the Directional Coupling method in combination with Average Power Sensing due to simplicity of their implementation [11].

The Directional Coupling method uses a special coupling, or interconnection technique, which implements a system such that a transmitting station can listen to all stations but itself, [12]. Collision detection in this system is straightforward. If a station senses data at its receiver while it is transmitting, it means that some other station is also transmitting and thus a collision has occured [11]. But, at the beginning of the receiving process, we do not have synchronization, thus no data bits can be recovered. To detect a collision we have to combine another method, namely Average Power Sensing, in which detection of the incoming signal is determined based on the average power it carries.

Synchronization of bursty traffic is solved by introducing a sinusoidal synchronization carrier that is sent through the fiber together with the data packet and switched on and off with it, [13]. The frequency of such a signal is 125 MHz, which is exactly the value where the Sinc shaped power spectral density of the encoded data signal has a first null. If the clock at the transmitter has been made from this sinusoidal signal it can easily be recovered at the receiver. Since the spectral content of data and synchronization signal do not overlap they can be easily separated at the receiver by means of filters. Note that we really need the preamble at the begining of the data packet in contrast to existing Fast Ethernet standards that do not require preamble of the packet due to the constant signaling they use.

Without going more into detailed description of the synchronization and collision detection we will now concentrate on the performance analysis of the network with respect to dispersion and attenuation.

2. Performance analysis of the systems with respect to attenuation and dispersion

The design of an optical system is a balancing act. The top two technical considerations are power budget and transmission capacity, or bandwidth. Power budget calculation is needed to assure that enough optical power reaches the receiver to give adequate performance. The calculation should leave some extra margin above the minimum receiver sensitivity to encounter system aging, fluctuations and repairs. However, the received power should not overload the receiver. The transmission capacity of an optical fiber system is the highest digital bit-rate it can carry [14]. In order to determine the transmission capacity we have to determine the dispersion effect in the system to assure the system can handle signals at the speeds we want to transmit.

To determine the effect of dispersion and attenuation on performance of presented systems we have made both analytical calculations and simulations using the program package MATLAB.

The result of the simulation either gives the maximum number of users in the mini-star and the number of mini-stars in the first architecture given the maximum bit rate of the signal it has to support, or the fiber length limitation due to dispersion and attenuation given the number of users per mini-star and the total number of users in the first architecture.

To simulate the attenuation limitation of the system calculation of received power based on transmitted power and losses in the system has to be done. Based on received power a maximum bit-rate that the system can support can be calculted based on the given sensitivity of the receiver (1). Moreover, calculation of the maximum bit rate the system can support based on dispersion has to be done to determine dispersion limitations of the system. Finally, based on the maximum bit-rate a system can support a fiber length limitation can be calculated from the bit-rate-distance product.

To calculate the maximum bit rate B_0 that a link of length L can transmit with a given BER the sensitivity of the receiver has to be specified. This is defined as the minimum number of photons per bit necessary to guarantee that the BER is smaller than prescribed rate. In our case BER=10^{-9}. A sensitivity of n_0 photons corresponds to an optical energy $h\nu n_0$ per bit and optical power [15]

$$P_p = 10.5\frac{h\nu n_0 B_0}{\eta} \quad (1)$$

where we assumed Poisson statistic of the photon arrivals. In (1) η is the quantum efficiency of the photodetector, which is for simulation purposes taken to be $\eta = 0.9$. For the receivers operating at λ_0=0.87 μm n_0 is approximately 300 photons per bit and this is the number we have used in our calculations.

The difference in calculating received power in two architectures is that WDM (de)multiplexer losses have to be taken into account in the first one. This means that in the second architecture we can either support more users or we can have a larger network span.

It is obvious that most of the losses in both architectures will be introduced by the passive star coupler. For simulation purposes we have used the expression for losses in the multimode integrated-optic polymer-based star coupler:

$$p_c = 10\log(N-1) + 4 \quad [\text{dB}] \quad (2)$$

where N is the total number of users in the mini-star interconnected by the star coupler. We have encountered in (2) measured propagation losses of 1.3 dB, fiber-chip coupling losses of 0.7 dB and mode dependent losses that are less than 2 dB. Note that $N-1$ is used in the expression due to a special construction of the star coupler.

Typical losses for the multimode fiber are 2.5 dB/km for wavelengths of optical light around 850 nm.

To calculate the system dispersion limitation we have used the procedure given in [16]. If the width of the received pulse that increases as the fiber length L increases exceeds the bit time interval $T = 1/B_0$, the performance begins to deteriorate as a result of intersymbol interference. Thus, to calculate the maximum fiber length that the pulse of a width T can travel along the fiber of length L that is used in the system we will use the expression for the bit-rate-distance product in the graded-index multimode fiber [16]

$$L \cdot B_0 = \frac{c_1}{\Delta^2} \quad [\text{km} \cdot \text{Mbps}] \quad (3)$$

where c_1 is the speed of light in the fiber and Δ is the fractional refractive index change in an optical fiber. For the fiber used in the systems $\Delta \approx 0.01$.

The losses of WDM (de)multiplexers are taken from the look-up table, which is made based on measurements [3]. These losses are included in the simulation of the first architecture.

Extra losses in the system that are included in the simulations are connector and splicing losses. Connector losses are taken to be 0.4 dB at maximum and splicing losses about 0.2 dB, which is a typical value that we have obtained from measurements.

The simulation results for the first architecture with 4 mini-stars and 16 users per mini-star is shown in Fig. 3. The emitted power was 0 dBm and receiver sensitivity -38 dB. Power margin is taken to be 3 dB.

It can be seen from the Fig. 3 that the maximum fiber length between any two computers in the system can be about L=1.3 km for the bit-rate B_0 of 125 Mbps, which is much larger than the length specified by the protocol [9, 10]. This means that fiber length will mostly be limited by the protocol and not by dispersion or attenuation. As we already predicted the main limitation in the system comes from attenuation.

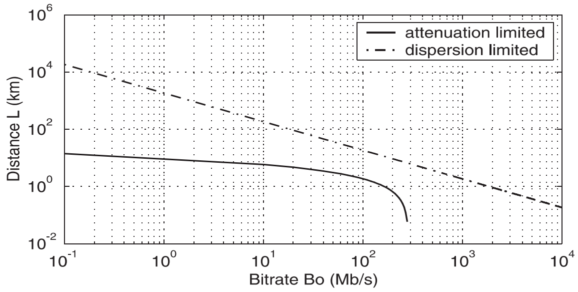

Figure 3. Maximum fiber length versus bit rate for the system with 4 mini-stars and 16 computers in the mini-star. Both attenuation in the system and dispersion in the fiber are taken into account.

The results of simulation for the second architecture is presented in Fig. 4.

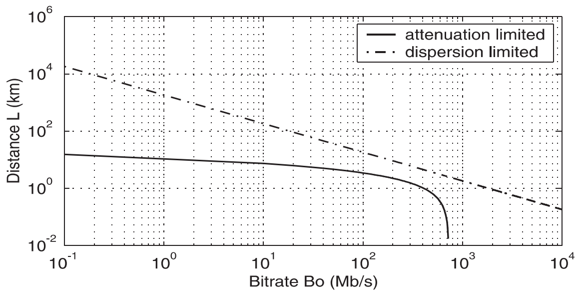

Figure 4. Maximum fiber length versus bit rate for the system with 16 computers in the mini-star. Both attenuation in the system and dispersion in the fiber are taken into account.

We see that the total fiber length can be larger since there are no WDM (de)multiplexer losses or we can have more users per mini-star.

To give more insight into the new PLD design we will present now the details of its digital part.

3. Digital part of the PLD

The digital part of the PLD has to accommodate signals coming from the MAC Layer via the MII for transmission and accept the specific signals from the analog part at reception and process it before proceeding it to the MAC layer. All the signals proceeded via the MII interface must follow the standard IEEE 803.2μ. The interface accommodates two 4-bit data buses and several control signals to cater for the communication need between the MAC and the Physical Layer [9]. There are several differences between the PLD in a 100BASE-T network and our new PLD.

First of all we do not use an IDLE signal for synchronization to avoid constant collisions. Moreover, we do not require a JAM signal, which is used by the hub to denote that some other station is transmitting commencing the collision detection process. This is due to the fact that we have here a point-to-multipoint connection and all the stations are sensing the shared medium at the same time. This will cause throughput increase in our networks, as will be shown later in this section. Another difference is that we do not need extra data encoding, like MLT-3 for example, in order to occupy less bandwidth, since we have enough bandwidth available in the optical fiber medium. Even data scrambling can be avoided. The preamble of the data packet is slightly changed due to the synchronization problem. Since the synchronization will not be established during the first several bytes of the data packet we cannot place a Start of Stream Delimiter (SSD) at the beginning of the packet, since it will not be detected. In the original standard this has been used to distinguish data packets from the IDLE signal. Thus, to detect the beginning of the packet the safest way is to put SSD just in front of the Start of Frame Delimiter (SFD), so we can be sure that the synchronization has been achieved at that point and that the packet can be recognized. This is shown in Fig. 5.

Another extra feature that we have inherited from the original 10BASE-T Ethernet is the Jabber Detection. This is important for disconnecting the end station that is continuously transmitting leading to a constant collision. After some predefined time, Unjab time, a station can be connected again. To disconnect a station a special signal is used that switches off the laser by decreasing its bias current. All the other functions stay the same. We have to stress that PLDs must have an internal clock running at 125 MHz that can be switched from a free-running value to the value determined by the incoming synchronization signal, which is specified by standard. This is important since we have a synchronization signal only during data packet duration.

There are some additional functionalities that are implemented in the design of the digital part of the PLD to provide testing facilities like the option to bypass scrambling/descrambling process in the transmitter and the receiver or the option to bypass the NRZI encoding/decoding process in the transmitter and the receiver and finally the option to perform loopback mode, i.e., the serial data output of the transmitter is feedback into the serial data input of the receiver.

Using a passive star coupler in both of the systems and possibility to avoid using JAM signal can affect increasing

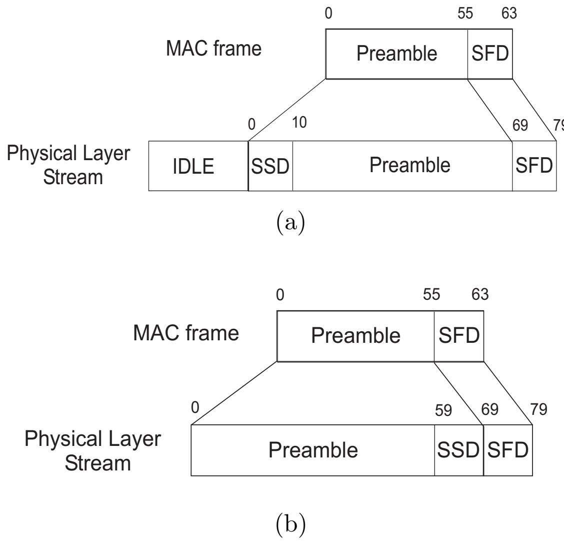

Figure 5. (a) IDLE signal and the Fast Ethernet data frame in the 100BASE-T standard, (b) Modified Fast Ethernet data frame: Start of Stream Delimiter is inserted just in front of the Start of Frame Delimiter to be sure that synchronization has been achieved.

the span and throughput in our network with respect to the ones specified in [9].

To determine maximum network span remind that the maximum propagation delay is the maximum round trip time taken by any two stations in the network and is defined to be 464 bit times (4.64 ms) [9]. Slot time, which corresponds to 512 bits, determines the upper bound on the acquisition time of the network and should be no longer than the sum of propagation time and the Jam time. It also restricts the length of the network. Since we do not use the Jam time we can afford to have longer propagation time, (512 bit times instead of 464), which results in a larger network span. The maximum delay caused by the cables and the other components in the signal path should not exceed the Slot time. Keeping this in mind the total delay is given by [5]:

$$\begin{aligned} \text{PDV} \quad = & \quad \text{link delays + repeater delays} \\ & + \text{DTE delay (NIC)+ safety margin} \end{aligned}$$

The DTE station is the first factor in determining the round trip delay. Since measured results of the new PLD are well within the limits of the specified value [9] the DTE delay does not exceed 25 bit times. The measured results for the delays in the digital part of the PLD will be given in the subsection 4.3.

The maximum delay caused by the standard 100BASE-T transmitter or receiver is 50 bit times [5]. What has remained is Slot time - Delay value of TX, RX, which is 412 bit times. As we do not have the delay caused by the repeater, we can consider this 412 bit times to be the maximum bound in calculating the network diameter. Having in mind bit time of 10 ns in the Fast Ethernet and the light propagation speed in fiber $(0.67 \cdot c)$ we have calculated that a maximum network span can be 412 m. We have also calculated the maximum permissible delay for this network length, and it turned out to be well within the limit of 512 bit times.

The calculated value of the maximum network span is 412 m, which is an advantage over the existing 100BASE-SX network, standardized by TIA/EIA as it can give a maximum of 300 m, [10].

Apart from increasing the network span, having no repeaters in the network and avoiding using the JAM signal can increase the throughput with respect to the 100BASE-T network [9]. In the existing Fast Ethernet networks the backoff algorithm starts by the transmitting stations after at least 64 bits of the preamble and 32 bits of the JAM time. Thus it takes at least 96 bit times. In our proposed scheme carrier sensing can be done well within the preamble time so collision detection can also be detected faster causing the backoff algorithm to start earlier. This may provide at least a slightly larger throughput than in the 100BASE-T networks.

To implement the digital part of the PLD we have used an FPGA chip form Altera APEX 20K chip family.

3.1. Transmitter

The block scheme of the transmitter is given in Fig. 6. Presented sub-modules run in two clock domains, namely 25 MHz and 125 MHz.

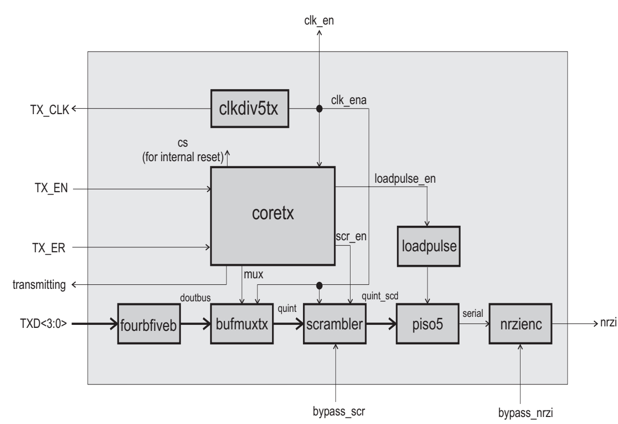

Figure 6. The transmitter block diagram.

Apart from the standardized signals that are coming from the MAC Layer as inputs to the transmiter we have introduced three more:

- clock: 125 MHz from the analog part of the PLD
- bypass_nrzi: Active-high static input signal to bypass NRZI encoding/decoding
- bypass_scr: Active-high static input signal to bypass scrambling

The presented output signals are also standardized [9].

The sub-modules, presented in Fig. 6 that run at 25 MHz are:

- **clkdiv5tx** - divides the 125 MHz nominal clock into 25 MHz. The output is connected to the TX_CLK output. It also provides clock enable signal, which is used by **coretx**, **bufmuxtx** and **scrambler**. This signal is also used by the jab counter and the unjab counter in the Jabber detection that is implemented apart from the transceiver.
- **fourbfiveb** - serves as the 4B/5B encoder. It encodes the TXD$\langle 3:0 \rangle$ into the code-groups.
- **bufmuxtx** - frame composer. It is controlled by the **coretx** via mux signal. It puts SSD, ESD and transmit-error code-groups into the frame when **coretx** signals it to do so. Otherwise, it will just pass the frame (which is already encoded by **fourbfiveb**). When no transmission, it simply outputs low signal.
- **coretx** - controller of other sub-modules. As such, it is a state machine. It takes TX_EN and TX_ER input signals, along with pre_count signal, which is internal to this sub-module (from internal counter), as the condition signals. The state machine runs by using the clock enable signal from **clkdiv5tx** sub-module.
- **scrambler** - performs parallel FSS scrambling on the data stream under **coretx** control. However, if the bypass_scr is asserted, it will not perform scrambling. It will just pass the data stream instead. Although it runs at 25 MHz its linear feedback shift register runs at 125 MHz.

The following sub-modules run at 125 MHz:

- **loadpulse** - produces a load signal that is used by **piso5** to load the parallel data stream into its shift registers. The **coretx** signals the **loadpulse** when to start producing the signal.
- **piso5** - parallel-to-serial converter, surely a shift register. The parallel data stream is loaded when the load signal is high. Then it will send out the serial data stream.
- **nrzienc** - encodes the serial NRZ data stream into NRZI format. However, if the bypass_nrzi is asserted, it will not perform NRZI encoding. It will just pass the data stream instead.

3.2. Receiver

A block scheme of the receiver is given in Fig. 7. Like in the transmitter, presented sub-modules run at two clock domains.

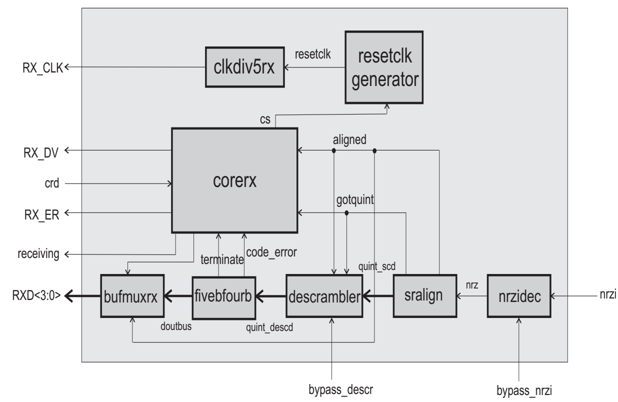

Figure 7. Block diagram of the digital part of the receiver.

The sub-modules that are presented in Fig. 7 are:

- **clkdiv5rx** - divides the 125 MHz nominal clock into 25 MHz. The output is connected to the RX_CLK output port. The **corerx** provides additional reset to this module to maintain such that the rising edge of RX_CLK is in the middle of RXD$\langle 3:0 \rangle$.
- **sralign** - composed of 10-bit shift register and a simple state machine. The function is to perform serial-to-parallel operation and to establish frame and byte alignment. The gotquint signal is a periodic pulse with 25 MHz frequency and will be used as the clock enable for the other sub-modules.
- **descrambler** - performs parallel descrambling on the data stream under **corerx** control. Upon detection of the SSD, the descrambler will be reset to a well defined initial state, after which it will start to descramble the rest of the incoming data. The SFD will be the first pattern to be descrambled. However, if

IEEE COMPUTER SOCIETY

no scrambling has been performed at the transmitting side the bypass_descr is asserted and this block will just pass the incoming data. Although this sub-module runs at 25 MHz its linear feedback shift register runs at 125 MHz.

- **fivebfourb** - converts the incoming (parallel) 5 bits quintets into corresponding (parallel) 4 bits nibbles. The use of 4B/5B coding in data transmission offers the possibility to send extra control codes along with normal data. As the code list does not contain control codes like stream delimiters, they cannot be decoded and must therefore be detected on beforehand. The full list of all data nibbles and their corresponding 5 bits quintets can be reviewed in [9]. When invalid code-groups are detected the **fivebfourb** will assert code_error signal otherwise, upon detection of the ESD code-groups, it will assert a terminate signal.

- **corerx** - controller of other sub-modules. As such, it is a state machine. It takes carrier detect (crd) input signal from the analog part of the receiver in the PLD, along with other signals indicated from the other sub-modules, i.e., aligned signal, code_error signal and terminate signal.

- **nrzidec** - decodes the incoming NRZ-I serial data stream into NRZ format. However, if the bypass_nrzi is asserted, it will not perform NRZI decoding. It will just pass the data stream instead. This block runs at 125 MHz.

- **bufmuxrx** - produces data stream that is connected to RXD$\langle 3:0 \rangle$ output port. It is controlled by **corerx**.

The output signal **receiving** is to denote that carrier is sensed (detected) and this will be used for collision detection together with the **transmitting** signal from the transmitter. Both signals are brought to the input of the AND gate with the collision detection signal COL at its output. If both signals are high, a collision detection signal COL will also be high indicating that collision has occured.

3.3. The time delay constraint

After realization of the digital part we have observed the timing delays of the design. To compare the obtained results with the ones given in the standard [9] we have produced Table 1.

It can be seen from this table that all the delay constraints from [9] are satisfied. These are used in the calculations to determine the maximum network span.

Table 1. Bit delay constraints: MDI to MII delay constraints (exposed MII, half duplex mode).

Sublayer measurement points	Event	Max (bits)
MII ⇔ MDI	TX_EN sampled to MDI output	8
	MDI input to CRS assert	17
	MDI input to CRS de-assert (aligned)	22 22
	MDI input to CRS de-asserted (unaligned)	17
	MDI input to COL assert	17
	MDI input to COL de-assert (aligned)	22
	MDI input to COL de-asserted (unaligned)	17

4. Experimental results

The experimental setup for both the transmitting and the receiving part of the PLD are shown in Fig. 8.

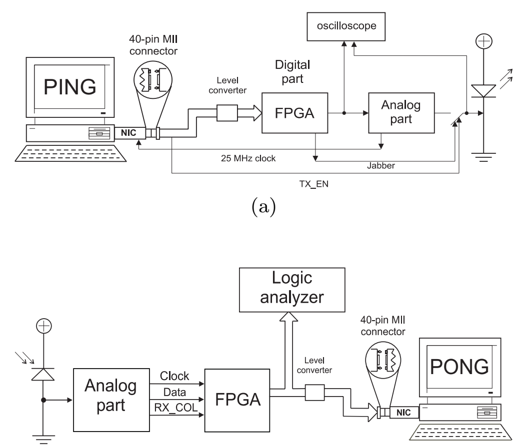

Figure 8. The experimental setup for both transmitting (a) and receiving part (b) of a new PLD.

To test the functionality of the digital part of the PLD we have performed the PING-PONG test between two computers. To simplify testing NRZI encoder has been bypassed as well as the scrambling. A data packet that is coming from the MAC Layer through the MII interface via the 4-line bus is brought to the FPGA input. This packet is accompanied by the clock (CLK), carrier sense (CRS) and management signals. The output of the FPGA is serial data that is to be transmitted over the fiber. This serial data signal is presented in Fig. 9.

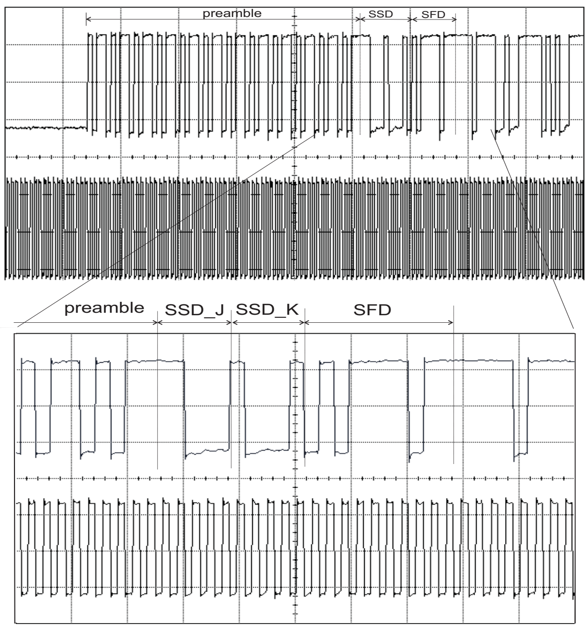

Figure 9. The serial data output from the FPGA chip.

As far as the receiver is concerned, once the clock and the data are recovered in the analog part, the FPGA processes the signal that is to be sent to the MAC Layer. This signal is presented in Fig. 10.

Received PONG signal on the screen of the receiving computer as a result of a PING request sent from the transmitting computer provided positive outcome of the experiments.

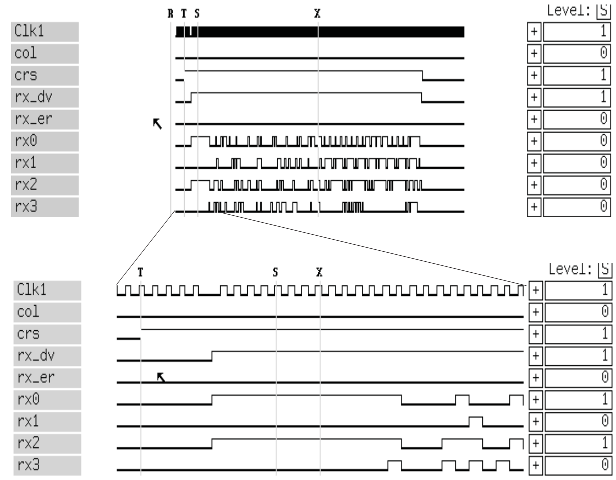

Figure 10. Parallel signals at the output of the FPGA to be transported to the MAC Layer via MII interface.

5. Conclusions and Discussions

Two LAN architectures for FTTD application are presented. Both architectures are based on the passive star coupler and accomodate Fast Ethernet protocol. We believe that they can be a solution for bringing fiber all the way to personal computers, especially in the environments "polluted" by the strong electromagnetic radiation. To minimize the cost we have based our networks on short-wavelength optical components, multimode optical fibers, multimode polymer-based integrated-optic devices and Fast Ethernet protocol. Performance analysis showed that the presented networks can have a larger span than specified in the 100BASE-SX standard. Since the first architecture is completely passive and so is most of the second one, we strongly believe that the Gigabit Ethernet protocol can run on those architectures requiring changes only in the NICs at the users site.

6. Acknowledgment

This work is a part of the MOUSE project sponsored by Dutch Technology Foundation (STW).

References

[1] N. Frigo, K. Reichmann, P. Iannone. "Whatever Happened to Fiber-to-the-Home?", in *Proceedings of OFC 2003*, paper TuR1, pp. 280-281, March, 2003.

[2] A. Savvas. "Fiber Networks: coming to a premises near you", *Lightwave Europe*, pp. 27–28, October, 2002.

[3] S. Musa, A. Borreman, G. Pandraud, P. Knijn, G. Sengo, M. B. J. Diemeer, A. Driessen. "Multimode fiber matched arrayed waveguides grating-based (de-)multiplexer for short distance communications," in *European Conference on Optical Communication*, Copenhagen, Denmark, PLC 6.2.1, September, 2002.

[4] S. Musa, N. S. Lagali, B. Docter, G. Sengo, G. J. M. Krijnen, A. Driessen. "Design and fabrication of low-cost, ultra-compact polymer based multimode 4 x 4 star couplers", in *10th European Conference on Integrated Optics (ECIO)*, Paderborn, Germany, pp. 248–251, 2001.

[5] C. E. Spurgeon. *Ethernet, The Definitive Guide*, USA: O'Reilly and Associates, Inc., February, 2000.

[6] L. B. Quinn, R. G. Russsell. *Fast Ethernet*. John Wiley & Sons, 1997.

[7] G. Held. *Ethernet Networks*. John Wiley & Sons, 1998.

[8] J. Genoe, D. Coppée, J. H. Stiens, R. A. Vounckx, M. Kuijk. "Calculation of the current response of the spatially modulated light CMOS detector", *IEEE Transactions on Electron Devices*, vol. 48, no. 9, pp. 1892–1902, September, 2001.

[9] IEEE Std 802.3. "Carrier Sense Multiple Access with Collision Detection (CSMA/CD) access method and physical layer specification", *Institute of Electrical and Electronic Engineering*. September, 1998.

[10] Optical Fiber Cabling Components Standard (ANSI/TIA/EIA-568-B.3-2000). [Online]. Available: http://www.tiaonline.org/ standards/

[11] J. W. Reedy, J. R. Jones. "Methods of Collision Detection in Fiber Optic CSMA/CD Networks", *IEEE Journal on Selected Areas in Communications*, vol. Sac3, pp. 890–896, November, 1985.

[12] T. Hermes. "New Reflective Type Star Coupler for Full Duplex Channels", *Electronics Letters*, vol. 27, pp. 2136–2138, November, 1991.

[13] I. Radovanović, W. van Etten. "New Ethernet Based Optically Transparent Network for Fiber-to-the-Desk Application", in *5th International Conference on Transparent Optical Networks (ICTON 2003)*, Warsaw, Poland, to be published.

[14] J. Hecht. *Understanding Fiber Optics*. Prentice Hall, 1999.

[15] W. van Etten, J. van der Plaats. *Fundamentals of Optical Fiber Communications,* Prentice Hall, New York, 1991.

[16] B. E. A. Saleh, M. C. Teich. *Fundamentals of Photonics,* John Wiley & Sons, Inc., 1991.